Phase control of spontaneous emission from a double-band photonic crystals*

Zhang Ke(张 珂)[a)b)], Zhu Yan-Ping(祝艳萍)[a)], Jiang Li(姜 丽)[a)], and Zhang Han-Zhuang(张汉壮)[a)†]

[a)] *College of Physics, Jilin University, Changchun* 130061, *China*

[b)] *Laboratory of Optical Physics, Institute of Physics, Chinese Academy of Sciences, Beijing* 100190, *China*

(Received 25 August 2008; revised manuscript received 24 August 2009)

Through the picture of dressed states, this paper investigates the spontaneous emission spectrum from a microwave-driven three-level atom embedded in double-band photonic crystals. The physical dynamics of the phase dependent phenomenon are analysed by comparing two models 'upper level coupling' and 'lower level coupling'. When the phase is changed from 0 to π, the variety of spontaneous emission spectra from either of the two models are inverse to each other, in which the relative height and width of the peaks are determined by the density of states in photonic crystals.

Keywords: photonic crystals, spontaneous emission, phase
PACC: 4250, 4270Q, 3290

1. Introduction

The process of spontaneous light emission is the collective quantum dynamics of electromagnetic radiation field and an atom. It has been shown that the modification and control of the spontaneous emission spectrum (SES) can be achieved by two aspects. On one side, atoms are put into photonic crystals (PCs) or the cavities, which have different densities of electromagnetic modes interacting with atoms. A narrow spectral line is presented in SES[1,2] and the upper state population reaches a steady state value with a slight oscillation.[3] On the other side, atoms are coupled with external coherent fields, especially to modulate the relative phases between the external fields.[4−6] Large enhancement or complete elimination of fluorescence spectra is achieved. Recently, many researchers are interested in controlling the spontaneous emission in a cavity varying the relative phase.[7,8] The threshold value is controlled and quantum logic devices will be realized in experiments.[9] Unfortunately, phase control of spontaneous emission from a double-band PCs has not been researched. In free space, the modification of the phase difference allows us to efficiently control the shape of the spontaneous emission spectrum and the population dynamics, which was explained by Knight,[10,11] and Martinez and Herczfeld.[12] However, in PCs, abrupt changes in the density of states (DOS) and photonic band gap (PBG)[13−15] may drastically modify the emission dynamics. These modifications can be viewed as long time memory effects and manifestations of non-Markovian behaviour in the atom-reservoir interaction.[16]

In this paper, we investigate the SES in the situation that the energy interval between the two close levels is smaller than the strength of external field. Then the two spectral structures $\alpha_{1,2}$ and $\beta_{1,2}$ locate in each side of the band gap in PCs. The different relative height and width of peaks in the SES are influenced by the DOS in different reservoirs. The width of the peaks in isotropic PBG is narrow in comparison with that in anisotropic PBG and vacuum, where SES are similar to each other. And the relative height changes as the variety of the different DOS. Then the origin of the phase dependence phenomenon, which is the consequence of the quantum interference, is described in detail. We found that the variety of the relative phase can bring oppositive influence on the two models. When the phase is changed from 0 to π, the two SES of each system are almost symmetrical with each other.

This paper is organized as follows. In Section 2, we derive the equations for describing the SES of the atom. In Section 3, the general calculated results and analysis of them are presented. The conclusions are summarized in Section 4.

*Project supported by the National Natural Science Foundation of China (Grant Nos. 10774060 and 10974071).
†Corresponding author. E-mail: hzzhang@mail.jlu.edu.cn
© 2010 Chinese Physical Society and IOP Publishing Ltd

2. The simplified models

In our model system, a three-level atom with the two close levels are driven by a microwave field of angular frequency with ω_0, Rabi frequency Ω_0, as shown in Fig. 1. The dipole allowed transitions are coupled by the same reservoirs, which are the isotropic PBG modes, anisotropic PBG modes and vacuum modes, respectively. The Rabi frequency Ω_0 is given by the product of the driving field amplitude and the phase term, $\Omega_0 = |\Omega_0|\mathrm{e}^{\mathrm{i}\,\phi}$. We assume that the phase of the pump laser field which is used to populate the upper levels is equal to zero, so the phase dependence is only related to the variety of the phase of the controlled laser field ϕ. The two models given in this paper are introduced as follows. The first one, as shown in Fig. 1(a), is 'lower level coupling' model, where the two close lower levels in a Λ-type atom are coupled by a microwave field. The second one, as shown in Fig. 1(b), is the 'upper level coupling' model. In this model two close upper levels in a V-type atom are coupled by a microwave field. The atom initially prepared in its excited states can decay spontaneously to the ground state through dipole-allowed transitions.

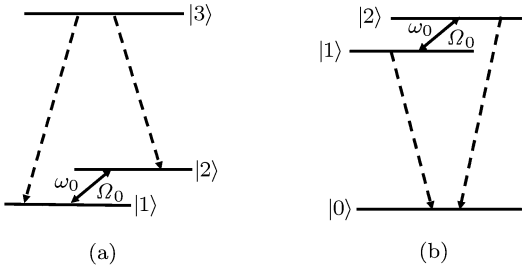


Fig. 1. Schematic representations of a driven three-level system: (a) for the 'lower level coupling', (b)for the 'upper level coupling'. The solid lines denote the microwave field, and the dash lines indicate the dipole allowed transitions.

The dispersion relations near the PBG edges are approximated by

$$\begin{cases} \omega_k = \omega_{\mathrm{c}1} - A_1(k-k_0)^2, & k < k_0, \\ \omega_k = \omega_{\mathrm{c}2} + A_2(k-k_0)^2, & k > k_0, \end{cases} \tag{1}$$

$$\begin{cases} \omega_k = \omega_{\mathrm{c}1} - A_1|(\boldsymbol{k}-\boldsymbol{k}_0)|^2, & |\boldsymbol{k}| < |\boldsymbol{k}_0|, \\ \omega_k = \omega_{\mathrm{c}2} + A_2|(\boldsymbol{k}-\boldsymbol{k}_0)|^2, & |\boldsymbol{k}| > |\boldsymbol{k}_0|, \end{cases} \tag{2}$$

$$\omega_k = ck, \tag{3}$$

for isotropic, anisotropic and vacuum dispersion relation, respectively. Here $A_n \approx \omega_{\mathrm{c}n}/k_0^2 \ \ (n = 1, 2)$, $\omega_{\mathrm{c}1}$ and $\omega_{\mathrm{c}2}$ are the upper and lower frequencies at the edges of the forbidden gap, respectively.

2.1. Equations for the SES of the 'lower level coupling'

In the interaction representation and the rotating wave approximation the interaction Hamiltonian can be written as:

$$H_{\mathrm{I}} = H_{\mathrm{A}} + H_{\mathrm{B}}, \tag{4}$$

$$H_{\mathrm{A}} = -\delta_0 \left|2\right\rangle\left\langle 2\right| + \mathrm{i}\,\hbar(\Omega_0 \left|2\right\rangle\left\langle 1\right| - \Omega_0^* \left|1\right\rangle\left\langle 2\right|), \tag{5}$$

$$\begin{aligned} H_{\mathrm{B}}^{\mathrm{l}} = {} & \mathrm{i}\,\hbar \sum_{k\lambda}[g_{k\lambda}^{31}(b_{k\lambda}^{\dagger} \left|1\right\rangle\left\langle 3\right| \mathrm{e}^{\mathrm{i}\,\delta_{k1}t} - \mathrm{H.c.}) \\ & + g_{k\lambda}^{32}(b_{k\lambda}^{\dagger} \left|2\right\rangle\left\langle 3\right| \mathrm{e}^{\mathrm{i}\,\delta_{k2}t} - \mathrm{H.c})], \end{aligned} \tag{6}$$

$$\delta_0 = \omega_0 - \omega_{21}, \quad \delta_{kj} = \omega_k - \omega_{3j}, \quad (j = 1, 2),$$

where H_{A} relates to the driving field. $H_{\mathrm{B}}^{\mathrm{l}}$ correlates with the interaction between models and reservoirs. The $b_{k\lambda}^{\dagger}$, $b_{k\lambda}$ are creation and annihilation operators for the kth mode with frequency ω_k. It should be noted that the superscript l denotes the operation in the 'lower level coupling',

$$g_{k\lambda}^{3j} = \frac{\omega_{3j} d_{3j}}{\hbar}\sqrt{\frac{\hbar}{2\varepsilon_0 \omega_k V}}\boldsymbol{e}_k \cdot \boldsymbol{d}_{3j}$$

is the frequency-dependent coupling constant between the atomic transition $|3\rangle \to |j\rangle$ and the mode $\{k\lambda\}$ of the radiation field.

We show that a convenient set of dressed atomic states paves the way to a much more natural description of the atomic dynamics. According to Eq. (5), we can obtain the dressed atomic eigenstates in both models,

$$\begin{aligned} \left|\alpha\right\rangle &= \sin\theta \left|1\right\rangle + \cos\theta\,\mathrm{i}\,\mathrm{e}^{\mathrm{i}\,\phi}\left|2\right\rangle, \\ \left|\beta\right\rangle &= \cos\theta \left|1\right\rangle - \sin\theta\,\mathrm{i}\,\mathrm{e}^{\mathrm{i}\,\phi}\left|2\right\rangle, \end{aligned} \tag{7}$$

and the corresponding eigenvalues are given by

$$\lambda_\gamma = -\frac{\delta_0}{2} \pm \sqrt{\left(\frac{\delta_0}{2}\right)^2 + |\Omega_0|^2}, \quad (\gamma = \alpha, \beta),$$

where

$$\sin\theta = \frac{|\Omega_0|}{\sqrt{|\Omega_0|^2 + |\lambda_\alpha|^2}}, \quad \cos\theta = \frac{|\Omega_0|}{\sqrt{|\Omega_0|^2 + |\lambda_\beta|^2}}.$$

So the expanded state vector of the system in the interaction picture can be written as

$$\begin{aligned} \left|\Psi^{\mathrm{l}}(t)\right\rangle = {} & C_3^{\mathrm{l}}(t)\left|3, 0\right\rangle \\ & + \sum_{k\lambda}[\alpha_{k\lambda}^{\mathrm{l}}(t)\left|\alpha, 1_k\right\rangle + \beta_{k\lambda}^{\mathrm{l}}(t)\left|\beta, 1_k\right\rangle]. \end{aligned} \tag{8}$$

Substituting Eqs. (4) and (8) into Schrödinger equation, $\mathrm{i}\,\hbar(\partial/\partial t)\,\Psi = H\,\Psi$, we obtain the equations of motion. The SES of the model, $S(\omega_k)$, is the Fourior transform of the equation,[17]

$$\langle E^-(t+\tau)E^+(t)\rangle_{t\to\infty} = \langle \Psi^{\rm l}(t)|\sum_{k,k\prime} b_k^\dagger b_{k\prime}\mathrm{e}^{\mathrm{i}\,\omega_k(t+\tau)}\mathrm{e}^{-\mathrm{i}\,\omega_{k\prime}t}|\,\Psi^{\rm l}(t)\rangle_{t\to\infty}. \tag{9}$$

From and Eqs. (8) and (9), we can obtain the SES

$$S^{\rm l}(\omega_k) \propto D(\omega_k)[\left|\alpha_{k\lambda}^{\rm l}(\infty)\right|^2 + \left|\beta_{k\lambda}^{\rm l}(\infty)\right|^2], \tag{10}$$

where $D(\omega_k)$ is the DOS of the radiation field, which can be derived as[16]

$$D(\omega_k) = \sqrt{\omega_k-\omega_{\rm c2}}\Theta(\omega_k-\omega_{\rm c2}) + \sqrt{\omega_{\rm c1}-\omega_k}\Theta(\omega_{\rm c1}-\omega_k), \quad \text{anisotropic PBG}, \tag{11}$$

$$D(\omega_k) = \frac{1}{\sqrt{\omega_k-\omega_{\rm c2}}}\Theta(\omega_k-\omega_{\rm c2}) + \frac{1}{\sqrt{\omega_{\rm c1}-\omega_k}}\Theta(\omega_{\rm c1}-\omega_k), \quad \text{isotropic PBG}, \tag{12}$$

$$D(\omega_k) = 1, \quad \text{vacuum}, \tag{13}$$

and

$$\begin{aligned}
\alpha_{k\lambda}^{\rm l}(\infty) &= -g_{k\lambda}^{31}\widetilde{C}_3^{\rm l}(s_{\alpha 1})\sin\theta + \mathrm{i}\,g_{k\lambda}^{32}\mathrm{e}^{-\mathrm{i}\,\phi}\widetilde{C}_3^{\rm l}(s_{\alpha 2})\cos\theta,\\
\beta_{k\lambda}^{\rm l}(\infty) &= -g_{k\lambda}^{31}\widetilde{C}_3^{\rm l}(s_{\beta 1})\cos\theta - \mathrm{i}\,g_{k\lambda}^{32}\mathrm{e}^{-\mathrm{i}\,\phi}\widetilde{C}_3^{\rm l}(s_{\beta 2})\sin\theta,\\
s_{\gamma j} &= -\mathrm{i}(\delta_{kj}+\lambda_\gamma),
\end{aligned} \tag{14}$$

where

$$\begin{aligned}
\widetilde{C}_3^{\rm l}(s) = \{&s + [(\widetilde{G}_{11}^{\alpha 1}+\widetilde{G}_{22}^{\beta 2})\sin^2\theta + (\widetilde{G}_{11}^{\beta 1}+G_{22}^{\alpha 2})\cos^2\theta] + \mathrm{i}[(\widetilde{G}_{12}^{\alpha 1}-\widetilde{G}_{12}^{\beta 1})\sin\theta\cos\theta\mathrm{e}^{\mathrm{i}\,\phi}\\
&+(\widetilde{G}_{21}^{\beta 2}-\widetilde{G}_{21}^{\alpha 2})\sin\theta\cos\theta\mathrm{e}^{-\mathrm{i}\,\phi}]\}^{-1}.
\end{aligned} \tag{15}$$

In the above equations

$$\widetilde{G}_{jl}^{\gamma j}(s) = \frac{1}{2}p_j p_l\eta_{jl}(\sqrt{-\mathrm{i}}\sqrt{s-\mathrm{i}\,\delta_{j\rm c1}-\lambda_\gamma} + \sqrt{i}\sqrt{s-\mathrm{i}\,\delta_{j\rm c2}-\lambda_\gamma}), \quad \text{anisotropic PBG}, \tag{16}$$

$$\widetilde{G}_{jl}^{\gamma j}(s) = \frac{1}{2}p_j p_l\eta_{jl}\left(\frac{\sqrt{\mathrm{i}}}{\sqrt{s-\mathrm{i}\,\delta_{j\rm c1}-\lambda_\gamma}} + \frac{\sqrt{-\mathrm{i}}}{\sqrt{s-\mathrm{i}\,\delta_{j\rm c2}-\lambda_\gamma}}\right), \quad \text{isotropic PBG}, \tag{17}$$

$$\widetilde{G}_{jl}^{\gamma j}(s) = \frac{1}{2}p_j p_l\eta_{jl}, \quad \text{vacuum} \quad (j,l=1,2),$$

they are the Laplace transforms of the delayed Green function

$$G_{jl}^{\gamma j}(t-t') = \sum_k g_{k\lambda}^{3j}g_{k\lambda}^{3l}\exp[-\mathrm{i}(\delta_{kj}+\lambda_\gamma)(t-t')],$$

and the definitions of the parameters are:

$$\begin{aligned}
\alpha_j &= \frac{1}{2\pi\varepsilon_0}\frac{\omega_j^2 d_j^2\omega_{\rm c2}^{1/2}}{3\hbar c^3}, \quad p_j = \sqrt{\alpha_j},\\
\beta_j^{3/2} &= \frac{1}{2\pi\varepsilon_0}\frac{\omega_j^2 d_j^2\omega_{\rm c2}^{3/2}}{3\hbar c^3}, \quad p_j = \sqrt{\beta_j^{3/2}},\\
\gamma_j &= \frac{2}{\pi\varepsilon_0}\frac{\omega_j^3 d_j^2}{3\hbar c^3}, \quad p_j = \sqrt{\gamma_j},
\end{aligned}$$

here, the parameters β_j and α_j^2 are the resonant frequency splittings[16] of anisotropic and isotropic PBG, γ_j is the effective decay rate for the transition from the upper level $|3\rangle$ to the lower level j in the vacuum reservoir.

The η_{12} is the coherent coupling coefficient of the transitions between $|3\rangle\to|1\rangle$ and $|3\rangle\to|2\rangle$ ($|2\rangle\to|0\rangle$ and $|1\rangle\to|0\rangle$ for the 'upper level coupling') coupled to the PBG and vacuum modes. So when $\eta_{12}=1$, namely, the associated dipoles are parallel or antiparallel, the two transition paths are tangled with each other and the quantum interference is maximal. And when $\eta_{12}=0$ meaning that the associated dipoles are orthogonal, there is no quantum interference between the two transitions. The parameter η_{jj} is independent of η_{12} and constantly equal to 1.[1]

The SES we obtained for the 'lower level coupling' is demonstrated in Fig. 2. Some necessary parameters are defined: $\delta_k = \omega_k - (\omega_{\rm c1}+\omega_{\rm c2})/2$ is the detuning of frequency of radiation field in the middle of the forbidden gap. $\delta_{\rm c2c1}$ is the width of the PBG, and $\delta_{jcl} = \omega_{3j} - \omega_{\rm cl}$ ($\delta_{jcl} = \omega_{j0} - \omega_{\rm cl}$ in 'upper level coupling').

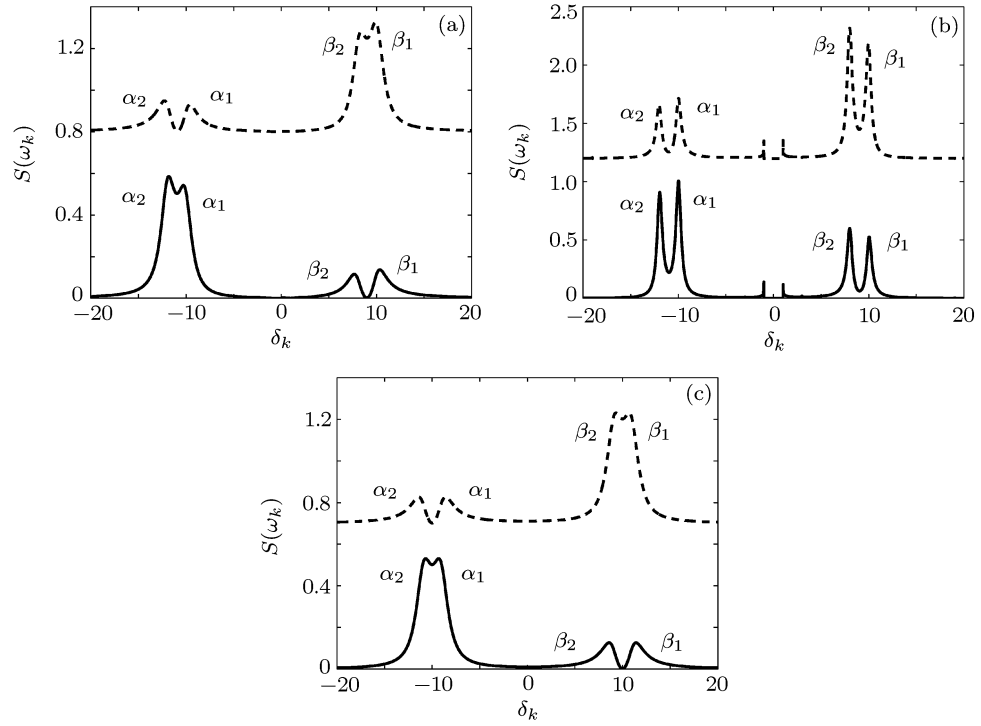


Fig. 2. The spontaneous emission spectrum $S(\delta_k)$ for the 'lower level coupling' as a function of detuning δ_k: (a) double-band anisotropic PBG reservoir; (b) double-band isotropic PBG reservoir; (c) vacuum reservior. The dash lines denote $\phi = 0$ while the solid lines denote $\phi = \pi$. The parameter $\eta_{12} = 1$ and the other parameters are $p_j = 1$, $\Omega_0 = 10$, $\omega_{21} = 2$, $\delta_{c2c1} = 2$, $\delta_{2c1} = -1$.

2.2. Equations for the SES of the 'upper level coupling'

For the 'upper level coupling', we make the similar calculations as the above part. The perturbed item in the Hamiltonian is

$$\begin{aligned} H_B^u &= \mathrm{i}\hbar\sum_{k\lambda}[g_{k\lambda}^{10}(b_{k\lambda}^{\dagger}|0\rangle\langle 1|\,\mathrm{e}^{\mathrm{i}\,\delta_{k10}t} - \mathrm{H.c.}) \\ &\quad + g_{k\lambda}^{20}(b_{k\lambda}^{\dagger}|0\rangle\langle 2|\,\mathrm{e}^{\mathrm{i}\,\delta_{k20}t} - \mathrm{H.c.})], \qquad (18) \\ \delta_{kj0} &= \omega_k - \omega_{j0}. \end{aligned}$$

It should be noted that the superscripts u denotes the operation in the 'upper level coupling', and

$$g_{k\lambda}^{j0} = \frac{\omega_{j0}d_{j0}}{\hbar}\sqrt{\frac{\hbar}{2\varepsilon_0\omega_k V}}\boldsymbol{e}_k\cdot\boldsymbol{d}_{j0}$$

is the frequency-dependent coupling constant between the atomic transition $|j\rangle\rightarrow|0\rangle$ and the mode $\{k\lambda\}$ of the radiation field. The expanded state vector is

$$\begin{aligned} |\Psi^u(t)\rangle &= \alpha^u(t)\,|\alpha,0\rangle + \beta^u(t)\,|\beta,0\rangle \\ &\quad + \sum_{k\lambda} C_{k\lambda}^u(t)\,|0,1_k\rangle\,. \qquad (19) \end{aligned}$$

So the SES can be written as

$$S^u(\omega_k) \propto D(\omega_k)|C_{k\lambda}^u(\infty)|^2, \qquad (20)$$

where

$$\begin{aligned} C_{k\lambda}^u(\infty) &= \mathrm{i}\,g_{k\lambda}^{20}\mathrm{e}^{\mathrm{i}\,\phi}[\alpha^u(s_2)\cos\theta - \beta^u(s_2)\sin\theta] \\ &\quad + g_{k\lambda}^{10}[\alpha^u(s_1)\sin\theta + \beta^u(s_1)\cos\theta], \\ s_j &= -\mathrm{i}\,\delta_{kj0}, \qquad (21) \end{aligned}$$

and the delayed Green function is defined as

$$G_{jl}(t-t') = \sum_{k\lambda} g_{k\lambda}^{\mathrm{j0}} g_{k\lambda}^{\mathrm{l0}} \exp[-\mathrm{i}\,\delta_{kj0}(t-t')].$$

The measurements of the delay function have become a major tool in quantum optics, which are determined by the radiation-field DOS. The SES for the 'upper level coupling' are given in Fig. 3.

3. Results and discussions

In order to minimize the algebraic labor we only take a resonant case that $\delta_0 = 0$ into consideration. In initial states, $C_3^{\mathrm{l}}(0) = 1$ and $\alpha^u(0) = \beta^u(0) = \sqrt{2}/2$.

We can obtain two dressed states $|\alpha\rangle$ and $|\beta\rangle$ which are generated by the quantum coherence in Eq. (7). From Eqs. (10) and (14) in the 'lower level coupling', we show the SES is shown in Fig. 2. The spectrum corresponding to $|\alpha\rangle$ is comprised of two lines α_1 and α_2, centred at $\omega_{31} - |\Omega_0|$ and $\omega_{32} - |\Omega_0|$. And the $|\beta\rangle$ is composed of two lines β_1 and β_2, centred at $\omega_{31} + |\Omega_0|$ and $\omega_{32} + |\Omega_0|$. From Eqs. (20) and (21), in the case of the 'upper level coupling', we show the SES in Fig. 3. The structures of two lines α_1 and α_2 are centred at $\omega_{20} - |\Omega_0|$ and $\omega_{10} - |\Omega_0|$. While β_1 and β_2 are centred at $\omega_{20} + |\Omega_0|$ and $\omega_{10} + |\Omega_0|$.[18]

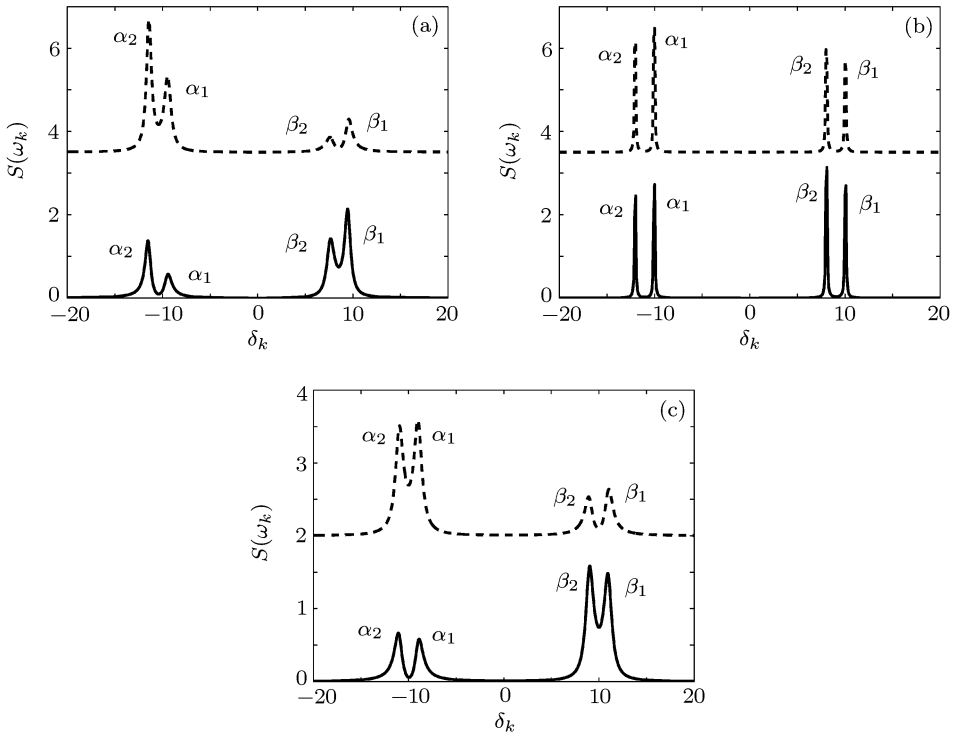


Fig. 3. The spontaneous emission spectrum $S(\delta_k)$ for the 'upper level coupling' as a function of detuning δ_k: (a) double-band anisotropic PBG reservoir; (b) double-band isotropic PBG reservoir; (c) vacuum reservoir. The solid lines denote $\phi = 0$ while the dash lines denote $\phi = \pi$. The parameter $\eta_{12} = 1$ and the other parameters are the same as Fig. 2.

In this paper, we only consider the situation $\omega_{21} < 2|\Omega_0|$ due to the small energy interval between two close levels $|1\rangle$ and $|2\rangle$. Thus the two spectral structures $\alpha_{1,2}$ and $\beta_{1,2}$ locate in each side of the band gap. Firstly, we investigate the character of the SES, especially including the relative height and width of peaks which are influenced by the DOS in different reservoirs. Obviously, the width of peaks in SES from anisotropic PBG and from vacuum are similar to each other. But the width of the peaks in isotropic PBG is narrower than that in anisotropic PBG and vacuum. The peaks also present different relative height due to different DOS. In the vacuum reservoirs as shown in Figs. 2(c) and 3(c), the two lines belonging to $|\alpha\rangle$ nearly have the same height, and the same is true for the components of $|\beta\rangle$. The character of SES in PCs displays different actions. For the anisotropic PBG, the DOS increases as the frequency is away from the band gap. Then in each pair of the peaks, such as the α_1 and α_2, the outside line α_2 is somewhat higher than the inside one α_1 as shown in Figs. 2(a) and 3(a). For the isotropic reservoirs, the DOS is very large on the edge of the band gap, and then decreases as the frequency is away from the band gap. So the outside line α_2 is smaller than the inside one α_1 in each pair as shown in Figs. 2(b) and 3(b).

Next we will demonstrate the quantum dynamics of the coupling of the external microwave field with an atom. From Eqs. (14) and (21), we obtain that there occurs a term $\eta_{12}e^{\pm i\phi}$, which plays an important role in our models. When $\eta_{12} = 0$, the quantum interference is absent. The SES have not any change as the phase, which can be seen from Fig. 4. So the phase dependence occurs only if $\eta_{12} \neq 0$. Namely, the phase sensitive phenomenon is the consequence of the quantum interference between the transition pathways $|3\rangle \rightarrow |1\rangle$ and $|3\rangle \rightarrow |2\rangle$ in the 'lower level coupling' and between the transitions $|1\rangle \rightarrow |0\rangle$ and $|2\rangle \rightarrow |0\rangle$ in the 'upper level

coupling'. When the phase is changed from 0 to π, the SES from the two models can vary as the phase in different tendency. For the 'lower level coupling', the phase dependent phenomenon are shown in Fig. 2. For the case that $\phi = \pi$ as shown by the dash lines, the height of the left side peaks $\alpha_{1,2}$ decreases with respect to the case that $\phi = 0$ as shown by the solid lines, while the right side peaks $\beta_{1,2}$ can be raised. For the 'upper level coupling', as shown in Fig. 3, the variety of height is inverse. Compared to the spectra of the two models, we found that the variety of the phase can bring oppositive influence on the two models. And the two SES of each system are almost symmetrical with each other.

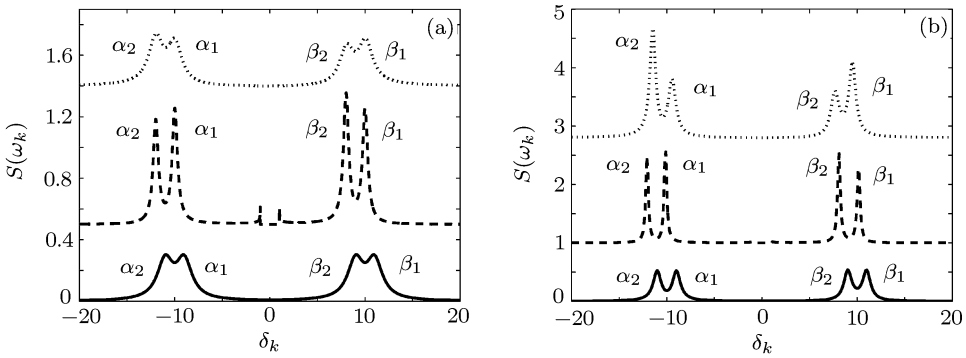


Fig. 4. The spontaneous emission spectrum $S(\delta_k)$ as a function of detuning δ_k when $\phi = 0$ and $\eta_{12} = 0$: (a) 'lower level coupling'; (b)'upper level coupling'. The dot lines are double-band anisotropic PBG reservoir, dash lines are double-band isotropic PBG reservoir, and the solid lines are vacuum reservoir. The other parameters are the same as those in Fig. 2.

In order to explicitly describe the interference between the two transitions from the excited level to the ground level, we take the example of the 'lower level coupling' to demonstrate the inherent characters of the phase dependence. And all transition pathways have been revealed in Fig. 5. Meanwhile, the physical implication of the term $\eta_{12}e^{\pm i\phi}$, which is raised by the driven field, would be interpreted. Then the quantum interference between the transition pathways $|3\rangle\rightarrow|1\rangle$ and $|3\rangle\rightarrow|2\rangle$ will be studied.

First, the interference between the transition in Fig. 5(b) and the one in Fig. 5(c) is independent of the variation of phase. It is only effected by η_{12}.

Secondly, the decay channel $|3\rangle\rightarrow|1\rangle\rightarrow|2\rangle$ is accompanied by the absorption of a microwave photon, as shown in Fig. 5(a), while the decay path $|3\rangle\rightarrow|2\rangle\rightarrow|1\rangle$ occurs with the emission of a microwave photon, as depicted in Fig. 5(d). Due to combining the absorption and emission of a microwave photon, the phase dependence in the interference between the two channels is canceled.

Thirdly, the phase dependence can only occur in two cases mentioned below. One case is the process of the interference between the transitions in Figs. 5(a) and 5(b). This process need emitting a microwave photon, as denoted by the factor $e^{i\phi}$. The other similar interpretation can be advanced for the interference between the transitions in Figs. 5(c) and 5(d). It is followed by the absorption of a microwave photon, as indicated by the appearance of the phase factor $e^{-i\phi}$.

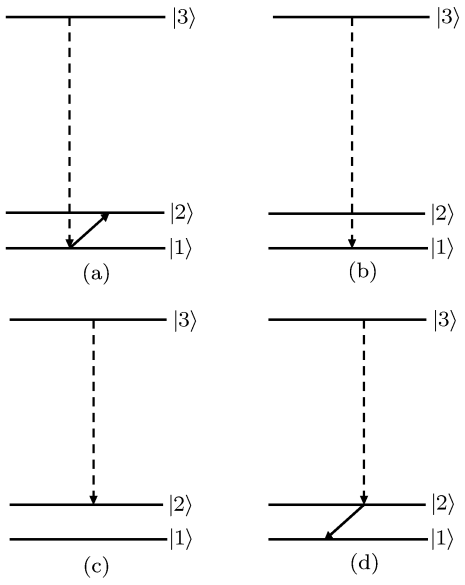


Fig. 5. The transition pathways of the model. (a) phase dependent interfering path is $|3\rangle\rightarrow|1\rangle\rightarrow|2\rangle$ via absorb a photon, (b)simple spontaneous decay $|3\rangle\rightarrow|1\rangle$, (c)simple spontaneous decay $|3\rangle\rightarrow|2\rangle$, (d)phase dependent interfering path is $|3\rangle\rightarrow|2\rangle\rightarrow|1\rangle$ via emission of a driving field photon.

4. Conclusion

In this article, using the relative phase we control the SES in PCs. In the situation that $\omega_{21} < 2|\Omega_0|$, the two spectral structures $\alpha_{1,2}$ and $\beta_{1,2}$ locate in each side of the band gap. The influence of the DOS is not the coupling of the laser fields with the atom but the phase dependent SES. The width of peaks in SES from anisotropic PBG and from vacuum are similar to each other. But the width of the peaks in isotropic PBG is narrower than that in anisotropic PBG and vacuum. The relative height is changed as the variety of different DOS. The interference between the decay pathways leads to the phase sensitive phenomenon. It is followed by the emission or absorption of a microwave field photon. For the 'lower level coupling', when the phase increases from 0 to π, the intensity of the lines $\alpha_{1,2}$ decreases, while the intensity of the lines $\beta_{1,2}$ increases. For the 'upper level coupling', the variety is contrary with the above case. When the change of the phase ϕ is equal to π, the spectra from either of two modes are almost a mirror image of each other.

References

[1] Zhang H Z, Tang S H and He J 2002 *Phys. Rev.* A **65** 063802
[2] Liu G Q, Wang J and Zhang H Z 2005 *Chin. Phys.* **14** 0102
[3] Sun X D, Jiang X Q and Hou C F 2007 *J. Phys.* B **40** 1645
[4] Ghafoor F, Zhu S Y and Zubairy M S 2000 *Phys. Rev.* A **62** 013811
[5] Li J H 2007 *Eur. Phys. J.* D **42** 467
[6] Hu X M, Shi W X, Xu Q, Guo H J, Li J Y and Li X X 2006 *Phys. Lett.* A **352** 543
[7] Settimi A, Severini S, Sibilia C, Bertolotti M, Napoli A and Messina A 2006 *Eur. Phys. J.* B **50** 379
[8] Osman K I 2006 *Opt. Commun.* **259** 194
[9] Fushman I 2008 *Science* **320** 769
[10] Gong S Q, Paspalakis E and Knight P L 1998 *J. Mod. Opt.* **45** 2433
[11] Paspalakis E, Keitel C H and Knight P L 1998 *Phys. Rev.* A **58** 4868
[12] Martinez M A G and Herczfeld P R 1997 *Phys. Rev.* A **55** 4483
[13] Yablonovitch E 1987 *Phys. Rev. Lett.* **58** 2059
[14] Liu Z Q, Feng T H, Dai Q F, Wu L J and Lan S 2009 *Chin. Phys.* B **18** 2383
[15] Chen Y Y, Huang Z M, Shi J L, Li C F and Wang Q 2007 *Chin. Phys.* **16** 173
[16] Woldeyohannes M and John S 1999 *Phys. Rev.* A **60** 5046
[17] Zhu S Y 1995 *Phys. Rev.* A **52** 710
[18] Yuan S and Gao J Y 2000 *Acta Phys. Sin.* **49** 1081 (in Chinese)